CMLS, Cell. Mol. Life Sci. 54 (1998) 196–202
1420-682X/98/020196-07 $ 1.50 + 0.20/0

CMLS Cellular and Molecular Life Sciences

Structural studies of a phosphatidyl serine-amorphous calcium phosphate complex

M. G. Taylor[a], K. Simkiss[a,] *, J. Simmons[a], L. N. Y. Wu[b] and R. E. Wuthier[b]

[a]School of Animal and Microbial Sciences, The University of Reading, Reading RG6 6AJ (United Kingdom), Fax +44 118 9316562
[b]Department of Chemistry and Biochemistry, The University of South Carolina, Columbia (South Carolina 29208, USA)

Received 14 November 1997; accepted 23 December 1997

Abstract. A phosphatidyl serine-amorphous calcium phosphate complex has been synthesized as a model of the matrix vesicle system that is associated with the induction of mineral deposition in bone, cartilage and dentine. The complex has been studied using a novel technique of subtractive extended X-ray absorption fine structure (EXAFS). This enables spectra of the components of the molecules to be subtracted from the complex so as to identify the sites of interaction. The results suggest there is a movement in the nitrogen atom of the phosphatidyl serine which approaches the calcium atom in the mineral phase. This interpretation would link the membrane structure of the vesicle to the structure of the mineral in a way that could explain some of its roles in biomineralization.

Key words. Phosphatidyl serine; biomineralization; membrane structure; EXAFS; calcium binding.

The formation and growth of biominerals is a complex process. At the chemical level it involves the control of supersaturation and ion activities which lead to the nucleation and growth of crystals [1]. In understanding many of these processes it is generally agreed that much depends upon the interactions that occur at the solid–solution interface of the component systems [2].

In many forms of biomineralization, lipid membranes or protein surfaces act as the sites for initial mineral deposition. This is certainly the case in the induction of mineralization in collagen-rich hard tissues such as bone, mineralizing cartilage and dentine [3]. In these tissues cell-derived, membrane-enclosed structures called matrix vesicles induce the primary mineralization by accumulating calcium and phosphate ions on the charged nucleating regions of the phospholipids that occur on their inner membrane surfaces [4]. These phospholipids appear to bind calcium as the initial step in the biomineralization process, and since phosphatidyl serine is concentrated in matrix vesicles [5, 6] and occurs particularly on the inner surface of these organelles, it has attracted particular interest [7].

The form of the mineral that is initially produced in the calcification process has been a source of considerable controversy. This arises partly because of the small size of these deposits and partly because of their poorly organized crystal lattice [5, 6]. In addition there have been different views as to the possible role of phosphatidyl serine in these processes. When dispersed in calcifying solutions, phosphatidyl serine induces hydroxyapatite formation both in vitro and in vivo. When included in liposomes, however, mineral formation is reduced. Since liposomes are often used as models of matrix vesicles, this has resulted in a number of suggestions about the multiple effects of phosphatidyl serine on the induction of bone formation [7].

In order to investigate this problem, we have used a phosphatidyl serine-amorphous calcium phosphate

* Corresponding author.

complex of the type that has been suggested as occurring at the sites of initial biomineralization in matrix vesicles [8]. This material has been studied by extended X-ray absorption spectroscopy (EXAFS) so as to obtain information about the atoms in the local environment around calcium. As a check on the consistency of the technique, the phosphorus K-edge was also measured. This provides an independent measure of the correspondence of Ca-P distances from the calcium edge and the P-Ca distances from the phosphorus edge. The technique of EXAFS uses a synchrotron radiation source to provide specific information on the type, number and distance of neighbouring atoms around a particular element. It will be apparent, however, that the interpretation of these data can be complicated since, in this specific case, it involves calcium binding by the lipid component as well as by the inorganic mineral. For the same reason there are two phosphate environments, one in the phospholipid and the other in the amorphous calcium phosphate.

In order to explore the environments around these atoms we developed a novel approach of subtracting the EXAFS spectra of the mineral component from that of the phosphatidyl serine-amorphous calcium phosphate complex and analysing the remaining component. By allocating the associated atoms to either the lipid or the mineral components, it should be possible to speculate on the possible nature of interactions between the two components.

Materials and methods

In order to interpret EXAFS spectra it is necessary to have model compounds of known composition and structure. Hydroxyapatite [$Ca_5(PO_4)_3OH$] was obtained from Fluka Chemicals (Gillingham, UK) and checked by powder diffraction. Amorphous calcium phosphate (ACP) was synthesized by the method of Mitchell et al. [9]. The ACP was prepared at pH 8, and the product was washed in water adjusted to pH 10 by the addition of sodium hydroxide. The product contained magnesium introduced as a crystal inhibitor to give a final Mg:Ca ratio of 0.07. The cation:phosphate ratio, however, was 1:1, implying that most of the phosphate was still protonated. The amorphous mineral contained 20% water.

The phosphatidyl serine–mineral sample was a lyophilized synthetic calcium-phospholipid-phosphate complex [8]. Freeze-drying did not affect the amorphous state of this material, which was checked using X-ray powder diffraction. There was a peak at 4.8 nm in the low-angle region, confirming the presence of lipid bilayers. In addition, there were some weak broad bands whose centres were close to those of the peaks found for hydroxyapatite. An infrared spectrum showed bands at 1030–1100 cm^{-1} assigned to P-O stretching vibrations and a band at 898 cm^{-1} indicating that the phosphate group was protonated [10]. The P-O antisymmetric bending mode showed some splitting with bands at 600 and 560 cm^{-1}. This splitting has been used to estimate the crystallinity of hydroxyapatite [11]. The ratios of calcium:inorganic phosphate:phosphatidyl serine were 1:1:1 as determined by analysis [8].

The short-range order in the material was studied by extended X-ray absorption spectroscopy of the calcium K-edge and the phosphorus K-edge using the Synchroton Radiation Source (SRS) at the Central Laboratories of the Research Councils (CLRC) at Daresbury, England. In this technique a photoelectron ejected from the K electron shell radiates out from the absorbing atom and is backscattered by the neighbouring atoms. The resulting interference between the outgoing and backscattered waves gives the fine structure of the X-ray absorption, from which very accurate assessments of interatomic distances can be determined.

Measurements of the calcium K-edge at 0.307 nm were made in transmission mode on Station 7.1 using powdered samples mounted in a flat sample holder with "Sellotape" windows, at ambient temperature and pressure. During the experiment the SRS ran with a circulating maximum beam current of 200 mA and an energy of 1.998 GeV. A silicon (111) monochromator was used, and harmonic contamination was minimized by running the ionization chambers semitransparent. As well as the calcium-phosphatidyl serine-phosphate sample, spectra were also measured of hydroxyapatite [$Ca_5(PO_4)_3OH$] and ACP. The spectra of these model compounds were measured and analysed to confirm the calculated phase shifts and assist in the analysis of the ACP and the calcium phosphatidyl serine phosphate (CaPSP).

For the measurements of the phosphorus edge an acetone slurry of the finely ground samples was mixed with graphite to make them more conducting in the beam, and mounted onto an aluminium holder. The measurements of the phosphorus K-edge at 0.579 nm were made at room temperature in vacuo at Station 3.4. using an InSb (111) crystal monochromator. The absorption was measured by total electron yield. The SRS conditions were the same as described above. The samples measured were the same as for calcium.

The total X-ray absorption, α, was obtained from the ratio of the transmitted (I_T) to incident (I_O) beam intensity:

$$I_T = I_O \exp(-\alpha t)$$

where t is the thickness of the sample.

Normalization and background subtraction of the spectra and analysis of the EXAFS spectra were done using the Daresbury library programs (EXCALIB, EXBACK and EXCURV92) [12, 13]. Phase shifts were calculated by ab initio methods in EXCURV92 for the central atom and for all the backscattering elements in the samples. Phase shifts arise as the photoelectron wave passes through the atomic potential of the emitting atom and is backscattered by the surrounding atoms. Interfer-

ence of these waves gives rise to the oscillations which make up the EXAFS experiment.

Results

The data for comparing the radial distribution functions and constructing a theoretical model for our fitting procedures for inorganic minerals were obtained from the Inorganic Crystal Structure Database (ICDS). Data on serine phosphate were obtained from the Cambridge Structural Database System (CSSR) kept at the Chemical Database Service at the CLRC laboratory at Daresbury. A crystal radial distribution calculation (CRAD) was made which gives the radial distribution and hence the local atomic environment about a user-defined central atom in a crystal structure. Each atom in the asymmetric unit can be computed separately to a specific range. The coordinates of the atoms are expanded by the space group symmetry and lattice translations to complete a sphere of defined radius which was then arranged in ascending order of distance.

A feature of calcium phosphate compounds is the range of bond lengths found in each coordination shell. Differences in coordination shell radii (r_{nm}) were therefore related to the data length, k in nm^{-1}, by the standard method [14], giving the EXAFS experimental resolution by

$$\Delta r_{nm} = \pi/(2k)$$

which for the data presented here is 0.01 nm. Models were constructed for both calcium and phosphorus environments by grouping bonds between the central absorbing atoms and the surrounding coordination shells.

Comparing the raw data obtained from the XANES (X-ray near-edge structure) of the calcium edge (fig. 1) which is sensitive to local symmetry, it is apparent that the calcium environment in the CaPSP complex is different from the model compounds. The position of the calcium K-edge itself at 4040 eV is the same for all the spectra within the instrumental resolution. This is to be expected for a Group II cation with a similar oxygen environment. Plotting the normalized weighted EXAFS spectra $\chi(k^3)$ against the wave vector, k (nm^{-1}) shows fine structure out to 8.0–10.0 nm^{-1}, and a signal-to-noise analysis [15] confirmed that the data were useful out to 10 nm^{-1}.

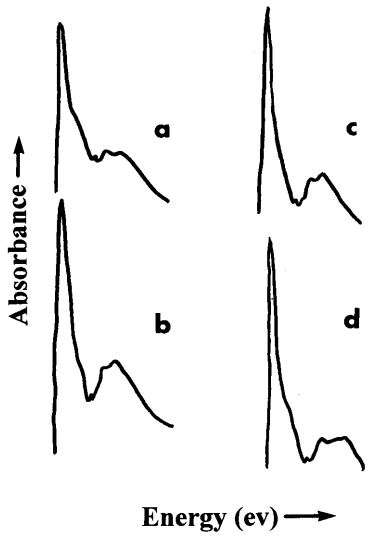

Figure 1. XANES (X-ray near-edge structure) spectra of (*a*) CaPSP complex compared with (*b*) monetite (*c*) ACP and (*d*) hydroxyapatite.

The phase shifts calculated with calcium as the central atom were checked against the crystallographic data of hydroxyapatite [16]. A theoretical model was constructed using the CRAD data for the number and type of atoms and the radii from the emitting to the scattering atoms in each shell.

The excellent fit of the calcium edge for hydroxyapatite is shown in figure 2 and the parameters used in the fitting are compared with the crystallographic data in table 1. Bond lengths are within 2% of the crystallo-

Table 1. EXAFS radial distribution function from the calcium K-edge for hydroxyapatite compared with the X-ray crystallographic data. EXAFS Debye-Waller factors $2\sigma^2$ are also included where σ is the relative mean square displacement in interatomic differences.

Coordination number	Atom type	X-ray shell radius/nm	EXAFS shell radius/nm	Debye-Waller factor $2\sigma^2/10^{-2}$ nm
4.0	O	0.239	0.234	0.015
2.5	O	0.247	0.250	0.013
2.0	O	0.277	0.282	0.038
2.5	P	0.320	0.321	0.040
1.5	O	0.342	0.349	0.002
1.0	Ca	0.344	0.344	0.014
3.0	P	0.360	0.353	0.028
5.5	O	0.395	0.400	0.037
5.0	Ca	0.399	0.401	0.032
3.0	Ca	0.414	0.418	0.013
4.5	O	0.432	0.426	0.004
2.0	O	0.448	0.453	0.009

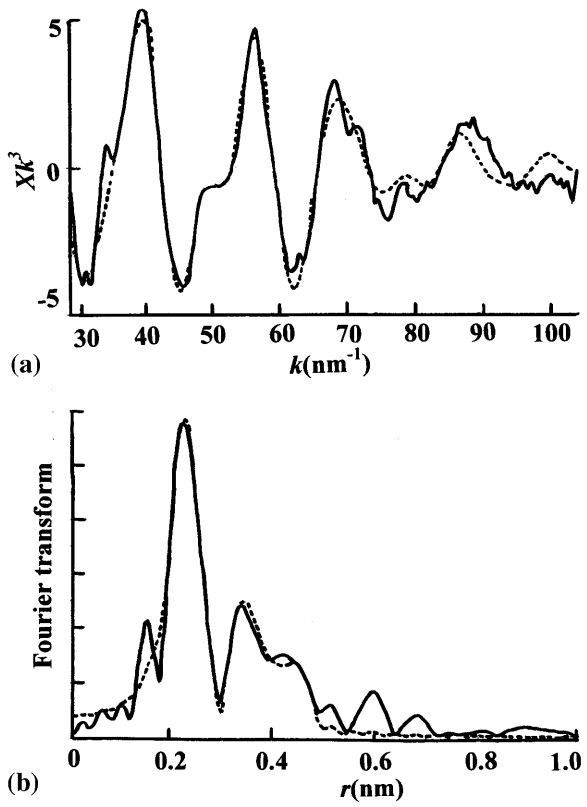

Figure 2. Calcium EXAFS spectrum for hydroxyapatite, compared with the X-ray crystallographic data [16]. (*a*) Weighted normalized EXAFS (k^3 Bohr radii^{-3}) for calcium K-edge. (*b*) Fourier transform of EXAFS from (*a*). Solid lines refer to the experimentally determined spectra, broken lines to calculated fits to X-ray data.

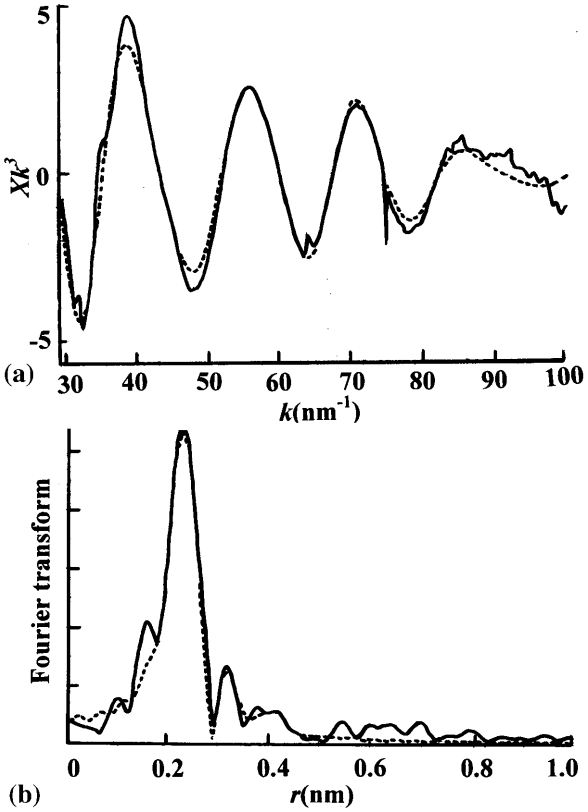

Figure 3. Calcium EXAFS spectrum for ACP. (*a*) Weighted normalized EXAFS (k^3, Bohr radii^{-3}) for calcium K-edge. (*b*) Fourier transform of EXAFS from (*a*). Solid lines refer to the experimentally determined spectra, broken lines to calculated fits.

graphic data, i.e. within the standard deviation from our averaging process. The first Ca-P shell at 0.321 nm compared with the P-Ca distance of 0.311 nm determined from the phosphorus K-edge. The second Ca-P shell was at 0.353 nm from the calcium edge, and the P-Ca distance from the phosphorus edge was 0.349 nm, well within the limits of the experiment. The analysis was performed to ca. 0.45 nm from the central atom, which is sufficient for our purposes in validating the phase shifts. Features in the EXAFS spectrum at 35 and 74 k (nm^{-1}) need shells to beyond 0.6 nm to be fitted [14]. Although there was some evidence for multiple scattering, with some very low Debye-Waller factors, we have confined our analyses throughout to the single scattering theory.

The lack of features in the EXAFS spectrum of ACP and the lack of strong peaks in the Fourier transform beyond 0.35 nm are typical of an amorphous compound. The spectrum was therefore fitted within that range. The EXAFS spectrum (fig. 3) has fewer features than that of crystalline hydroxyapatite, and the parameters were allowed to float for fitting with a least-squares procedure. The first Ca-O shell distance settled at 0.234 nm and in fact was the same as that found for hydroxyapatite. A Ca-P shell is present at 0.309 nm in both the calcium edge and phosphorus edge spectra, and the similarities in these distances in the different experiments give confidence in the analyses and calculated phase shifts.

The EXAFS spectrum and Fourier transform of the CaPSP sample differ from those of the model compounds, but there are some structural features in the EXAFS which are similar to those found in the hydroxyapatite spectrum (fig. 4). The Fourier-transformed spectrum in real space shows the first shell Ca-O peak with a distinct shoulder on the high side which is not seen in the model compounds or ACP. This suggests that the calcium is in a much more complicated environment than in the simpler calcium phosphates. The analytical data of the CaPSP complex showed that the Ca:PS:P_i was 1:1:1, indicating that calcium was bound to groups on the phosphatidyl serine as well as to the phosphate groups of the ACP. The EXAFS spectrum of ACP was therefore subtracted from the spectrum of the CaPSP sample. This procedure involves estimating the relative proportions of

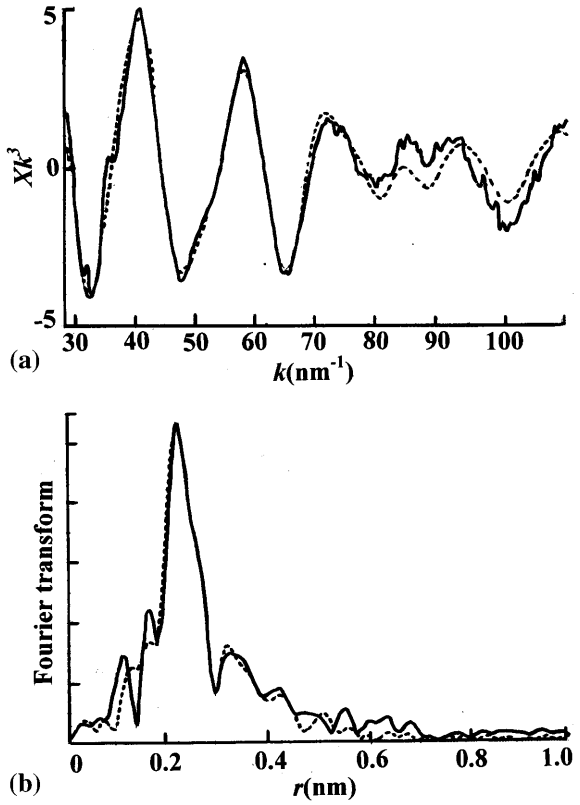

Figure 4. Calcium EXAFS spectrum of CaPSP. (*a*) Weighted normalized EXAFS (k^3, Bohr radii^{-3}) for calcium K-edge. (*b*) Fourier transform of EXAFS from (*a*). Solid lines refer to the experimentally determined spectra, broken lines to a calculated spectrum derived from combining the spectra of ACP (fig. 3) and CaPS (fig. 5). See text for details.

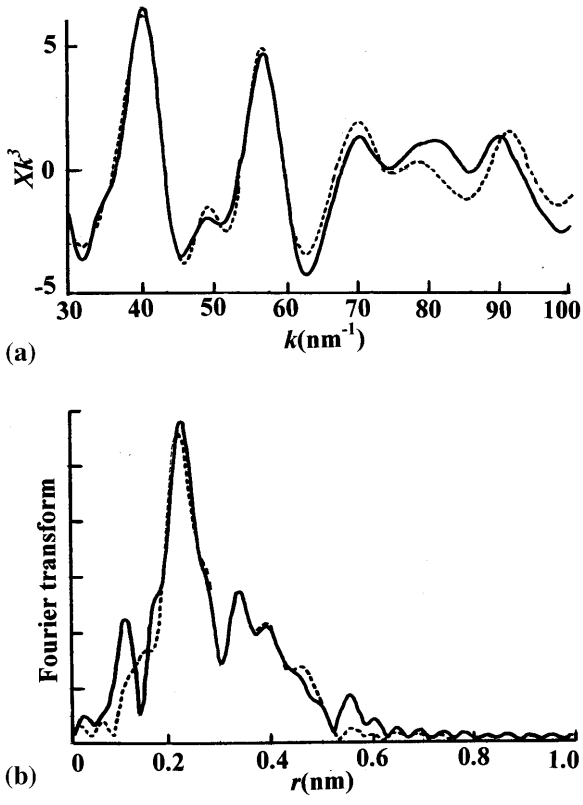

Figure 5. Calcium EXAFS spectrum of the CaPS component of the complex. (*a*) Back-transformed EXAFS spectrum of calcium K-edge. (*b*) Fourier transform of (*a*). Solid lines refer to the subtracted component and broken lines to the calculated fit.

each component, which from the analytical data is 1:1. Since the EXAFS spectrum is normalized to one emitting atom to give the radial distribution function, the ACP spectrum was multiplied by 0.5 before it was subtracted from the total spectrum. Both spectra were aligned before subtraction. The remaining spectrum, which was considered to result from the phosphatidyl serine component, was then multiplied by 2 to restore the normality. To verify the assumption that the inorganic and organic phosphates were present in equal ratios, a series of subtractions were made using various proportions of ACP to see which combination gave the best fit. Accordingly 0.3, 0.4, 0.6 and 0.7 ratios were also subtracted, but the 0.5 ratio gave the best fit. It was immediately apparent that the peak seen on the high side of the first major peak in the Fourier-transformed spectrum (fig. 4b) was associated with the phosphatidyl serine component. The residual spectrum was Fourier-filtered from 0 to 50 nm and then back-transformed from real space to 'k' or reciprocal space for analysis, assuming that the calcium was bound to the hydrophilic region of phosphatidyl serine (fig. 5). No crystallographic data are available for such a complex or for a calcium serine phosphate. X-ray data are, however, available for crystalline serine phosphate [17], calcium acetate [18], calcium EDTA and calcium NTA complexes [19], and these data were therefore used to construct a model of this component. On this basis the calcium appears to be bound to both the carboxylate and the phosphate ester groups. Support for calcium binding to the carboxylate group was gained by comparing our results with the calcium acetate crystal structure. The Ca-O distances in the first shell of our CaPS component are at 0.228 nm, which is similar to the first shell distance for calcium acetate. A shell of carbon at 0.297 nm also matches the distance of 0.329 ± 0.023 nm at the first calcium site. The fitting in this model improved by including a shell with nitrogen at 0.344 nm. This distance is considered reasonable, since in free phosphatidyl serine the amine and carboxylate groups carry charges, but with the electrostatic interaction of calcium with carboxylate there is a loss of the zwitterionic properties which allows the nitrogen to approach calcium. A similar situation occurs in calcium EDTA

Table 2. EXAFS radial distribution function of the calcium K-edge for CaPSP sample: two-component analysis based on stoichiometry. $Ca:PS:P_i$ ratio = 1:1:1 consisting of (i) CaPS component and (ii) ACP. EXAFS Debye-Waller factors, $2\sigma^2$, are also included where σ is the relative mean square displacement in interatomic distances.

Sample	Coordination number	Atom type	Shell radius/nm	Debye-Waller units $2\sigma^2/10^{-2}$ nm
CaPSP	2.2(5)	O	0.229	0.007
	4.5	O	0.247	0.023
	1.0	O	0.286	0.009
	1.7(5)	C	0.313	0.037
	1.7(5)	P	0.318	0.024
	1.5	Ca	0.331	0.020
	1.5	O	0.338	0.012
	1.0	N	0.342	0.013
	2.5	C	0.399	0.012
	1.5	Ca	0.419	0.050
	2.5	O	0.443	0.027
	1.0	Ca	0.488	0.023
CaPS(1)	2.5	O	0.228	0.010
	5.0	O	0.244	0.033
	3.0	C	0.297	0.007
	1.0	P	0.322	0.044
	2.0	Ca	0.342	0.029
	1.6	N	0.344	0.035
	4.0	C	0.392	0.010
	3.0	Ca	0.413	0.026
	3.1	O	0.445	0.059
	2.0	Ca	0.473	0.023
ACP(2)	2.0	O	0.234	0.013
	4.0	O	0.246	0.029
	2.0	O	0.288	0.025
	2.5	P	0.309	0.039
	1.0	Ca	0.320	0.026
	2.0	O	0.327	0.023
	2.0	O	0.425	0.041

complexes where calcium comes within 0.270 nm of a nitrogen atom. The results of this analysis are shown in figure 5 and table 2. The results of the analyses of the ACP and CaPS components were then combined and compared with the original CaPSP spectrum. The parameters were scaled to take account of the normalization of one calcium in the original spectrum, and after final optimization the results were compared in table 2. Comparison of these parameters with the experimental spectrum of CaPSP is shown in figure 4, where the goodness of the fit supports this model.

Discussion

Matrix vesicles are thought to arise by budding from the cell membranes of chondroytes, osteoblasts and odontoblasts. They are apparent as extracellular, 100-nm, membrane-enclosed particles that are associated with the initial sites of calcification [20]. The formation of hydroxyapatite crystals occurs in association with the inner surface of these vesicles, which eventually rupture and produce spherulitic growth at these extracellular sites [6]. The membranes of matrix vesicles have a characteristic composition [5] that has led to speculation about the involvement of acidic phospholipids and especially phosphatidyl serine in mineral nucleation and growth [21]. Thus, when free in solution, phosphatidyl serine facilitates the formation of hydroxyapatite from appropriate solutions, but if bound into a membrane it inhibits this process [7]. When incorporated into artificial liposomes, it is possible to model normal matrix vesicle behaviour in that the phosphatidyl serine facilitates intravesicular calcification at the expense of mineral deposition externally [22, 23]. The extent of this inhibition is correlated with the strength of the electrostatic interaction between the polar head group of the phospholipid and the surface of the mineral phase [21].

The results of the present study are relevant to these models. Thus, by separating the spectrum of the amorphous CaPSP complex into its separate components, it is possible to identify the molecular configurations that occur at the site of this interaction. Our data are indicative of a conformational change in the phosphatidyl serine when it is in association with a calcium atom in the mineral phase. This change is not specific to hydroxyapatite crystals, but includes amorphous calcium phosphates which may act as precursors to the crystalline phase. The nature of this hitherto unexpected change appears to be due to the movement of the nitrogen atom of the phosphatidyl serine toward the calcium atom. This apparently occurs because the charges on the phospholipid carboxyl group and the adjacent protonated nitrogen are reduced during this interaction.

Acknowledgements. We thank the Engineering and Physical Sciences Research Council for support (JS), A. J. Dent for assistance with the spectral subtraction procedures and the staff of the Synchrotron Radiation Source for use of the facility.

1 Simkiss K. and Wilbur K. W. (1989) Biomineralization, Academic Press, San Diego
2 Mann S. (1988) Molecular recognition in biomineralization. Nature **332:** 119–124
3 Plate U., Tkotz T., Wiesmann H. P., Statmann V., Joos U. and Hohling H. T. (1996) Early mineralization of matrix vesicles in the epiphyseal growth plate. J. Microscopy **183:** 102–107
4 Hohling H. J., Arnold S., Barkhaus R. H., Plate U. and Wiesmann H. P. (1995) Structural relationship between the primary crystal formations and the matrix macromolecules in different hard tissues. Discussion of a general principle. Con. Tissue Res. **33:** 171–178
5 Wuthier R. E. (1975) Lipid composition of isolated cartilage cells, membranes and matrix vesicles. Biochim. Biophys. Acta **409:** 128–143
6 Christoffersen J. and Landis W. J. (1991) A contribution with review to the description of mineralization of bone and other calcified tissues in vivo. Anat. Rec. **230:** 435–450
7 Boskey A. L. and Dick B. L. (1991) The effect of phosphatidyl-serine on in vitro hydroxyapatite growth and proliferation. Calcif. Tissue Intern. **49:** 193–196
8 Cotmore J. M., Nichols G. and Wuthier R. E. (1971) Phospholipid–calcium phosphate complex: enhanced calcium migration in the presence of phosphate. Science **172:** 1339–1341

9 Mitchell P. C. H., Parker S. F., Simkiss K., Simmons J. and Taylor M. G. (1996) Hydrated sites in biogenic amorphous calcium phosphates: an infrared, Raman and inelastic neutron scattering study. J. Inorg. Biochem. **62:** 183–197
10 Wu L. N. Y., Genge B. R., Dunkelberger D. G., LeGeros R. Z., Concannon B. and Wuthier R. E. (1997) Physiochemical characterization of the nucleational core of matrix vesicles. J. Biol. Chem. **272:** 4404–4411
11 Blumenthal N. C., Posner A. S. and Homes J. M. (1972) Effect of preparation conditions on the properties and transformation of amorphous calcium phosphate. Mat. Res. Bull. **7:** 1181–1190
12 Gurman S. J., Binsted N. and Ross I. (1984) A rapid exact curved-wave theory for EXAFS calculations. J. Phys. (Paris) **C17:** 143–151
13 Gurman S. J., Binsted N. and Ross I. (1986) A rapid, exact curved-wave theory for EXAFS calculations II. The multiple-scattering contributions. J. Phys. (Paris) **C19:** 1845–1861
14 Harries J. E., Hukins D. W. L. and Hasnain S. S. (1986) Analysis of the EXAFS spectrum of hydroxyapatite. J. Phys. (Paris) **C19:** 6859–6872
15 Dent A. J., Stephenson P. C. and Greaves G. N. (1992) The extraction of signal to noise values in x-ray absorption spectroscopy. Rev. Sci. Instrum. **63:** 856–858
16 Kay M. I., Young R. A. and Posner A. S. (1964) Crystal structure of hydroxyapatite. Nature **204:** 1050–1052
17 Sundaralingham M. and Putkey E. F. (1970) Molecular studies of amino acids and peptides II. A redetermination of the crystal structure of L-O-serine phosphate. A very short phosphate-carboxyl hydrogen bond. Acta Crystal. **B26:** 790–800
18 Klop E. A., Schouten A., Van der Sluis P. and Spek A. L. (1984) Structure of calcium acetate monohydrate, $Ca(C_2 H_3 O_2)_2 H_2O$. Acta Cryst. **C40:** 51–53
19 Barnett B. L. and Uchtman V. A. (1979) Structural investigations of calcium-binding molecules. Calcium binding to amino carboxylates. Crystal structures of Ca(CaEDTA). $7H_2O$ and Na(CaNTA). Inorg. Chem. **18:** 2674–2678
20 Anderson H. C. (1995) Molecular biology of matrix vesicles. Clin. Orthop. **314:** 266–280
21 Eanes E. D. (1989) Biophysical aspects of lipid interaction with mineral: liposome model studies. Anat. Rec. **224:** 220–225
22 Skrtic D. and Eanes E. D. (1992) Membrane-mediated precipitation of calcium phosphate in model liposomes with matrix vesicle-like lipid composition. Bone Miner. **16:** 109–119
23 Eanes E. D. (1992) Mixed phospholipid liposome calcification. Bone Miner. **17:** 269–272